



Ultimate bearing capacity of MV piles derived from load tests, a suggested new design approach

Rodriaan Spruitⁱ⁾, Ken Gavinⁱⁱ⁾, Jan van Dalenⁱ⁾, Rien Polakⁱⁱⁱ⁾, Jan Putteman^{iv)}, Alfred Roubos^{v)} and Frederike Westerbeke^{iv)}

i) Geotechnical Consultant, Department of City Development, Municipality of Rotterdam, Rotterdam, the Netherlands

ii) Professor, Department of Civil Engineering, Delft University of Technology, Delft, the Netherlands.

iii) Geotechnical Consultant, Volker Staal en Funderingen, Dordrecht, the Netherlands.

iv) Geotechnical Consultant, Engineering department, SBE Nederland, Rotterdam, the Netherlands

v) Senior Project Engineer, Port of Rotterdam, Rotterdam, the Netherlands

ABSTRACT

Driven steel beams with grout injection (MV-piles) are since the 80's in use in the Rotterdam harbour to deliver tension bearing capacity for anchoring large deep-sea quay walls.

This paper discusses the results from pile load tests on two sites within a historical context of port development and evolving load tests. The tested tension piles were fully instrumented with fiber optic strain sensors allowing for capturing a continuous strain profile along the full length of the piles. Practical information on instrumentation, testing and interpretation will be illustrated with actual test results.

Keywords: tension pile, load test, bearing capacity, distributed strain measurement, BOTDR, BOTDA, CPT based design

1 INTRODUCTION

The Port of Rotterdam is one of the largest ports in the world. Major deep-sea quay walls are currently being constructed in a vast area of reclaimed land, Maasvlakte II. The quay walls are founded in very dense Pleistocene Sand layers, however, the soil-retaining heights required for modern vessels are such that tension anchors with fairly high load capacity are required. Driven steel H-shaped beams with grout injection (MV piles) are used in most projects in the port since the 1980's. As a result of detailed load-test programmes, the design method for these anchors has developed over the years.

In Dutch practice, the ultimate bearing capacity (tension shaft resistance, τ_f) is correlated directly to the Cone Penetration Test (CPT), end resistance, q_c using a factor $\alpha_t = \tau_f / q_c$. Back-analyses of anchor-load tests suggests constant α_t factors in the range 1.2 - 1.4% of q_c . These values are usually limited to a maximum τ_f of approximately 250 kPa, corresponding in effect to a

limiting CPT-based q_c value of between 18 - 21 MPa. These limiting CPT values are higher than the limiting q_c value of 12- 15 MPa used in the rest of the Netherlands because of the history of load testing performed in the port of Rotterdam. This paper shows that as the ships have grown larger, retained heights of quay walls have increased. The expansion of the harbour into the North Sea has meant the soil strengths encountered have also increased, with q_c values in the range 40 - 80 MPa commonly encountered. In a competitive domain, such as port infrastructure it is vital that the design of all components of costly infrastructure are optimised.

Between 2018 and 2021 eight load tests were performed by the municipality of Rotterdam (department of City Development) at two sites in the Maasvlakte port district. The failure loads from these tests were on average 10 MN. The tests allowed detailed strain distributions along the full length of the test piles and as

a result offer the possibility to accurately determine the local mobilisation of shaft friction in addition to the ultimate failure load. Apart from describing the successful instrumentation with optical fibres (Brillouin Optical Time Domain Analysis (BOTDA) technique), the paper also addresses the test results in detail. The test results include load-displacement curves, creep behaviour and the strain distributions along the full length of the test piles for each load step. Illustrated with these test results, recommendations will be provided on how to optimally take advantage of the measurements during the test and when interpreting the data.

The improved understanding of friction development, including softening effects, that results from the strain distribution measurements, opens the route to an improved design method. In-house software that simulates the load-displacement behaviour of the load tests was used to evaluate the test results. The benefits of soil-structure interaction models will be discussed for the simulation of load tests and for design purposes.

The paper will conclude with: (1) detailed recommendations on pile instrumentation using optical fibres for BOTDA-distributed strain measurements, including novel techniques and practical tips and tricks, (2) how to determine ultimate friction from CPT data and finally, (3) how mobilisation of local friction along the pile can be modelled in soil-structure interaction simulation software.

2 DEVELOPMENT OF THE PORT OF ROTTERDAM

As most towns in the Netherlands the origin of Rotterdam can be traced back till around the 9th century when Rotta was only a small fishermen's settlement at the confluence of the small river Rotte in the Meuse. To be relatively safe for flooding, the settlement was located about 20 km inward along the river. Around 1270 a dam in the river Rotte was built, the origin of the city name. In 1299 city rights were established for the first time, to be reinstalled in 1340. The city wall was erected in 1360.

The first quay walls started to be built around the same time, along the harbour channels in the city centre. Those quay walls were constructed with an upper part of masonry, founded on a wooden platform on timber piles.

The first main boost for the Port of Rotterdam was the excavation of the 'Nieuwe Waterweg' (new waterway) that straightened and deepened the Meuse estuary. This channel was completed in 1872.

With the rapid post-war development of the Rotterdam harbour towards the coast, the amount of quay-wall length increased from 15 km before the second world war till the current 80 km total length of quay walls.

At the same time, the retaining height of the quay

walls (to allow for deeper draught for larger vessels) increased roughly from 15 m to 30 m (see Fig. 1).

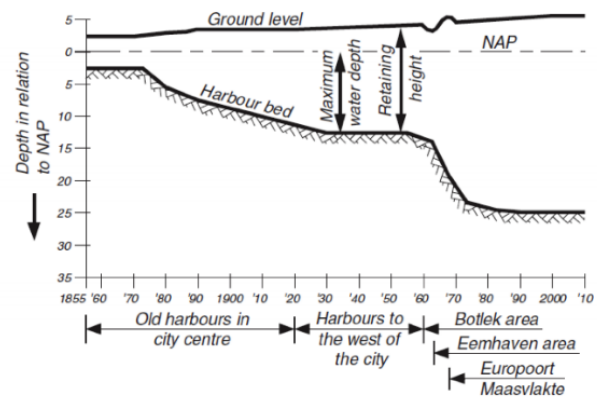


Fig. 1: Development of harbour depth and retaining height (De Gijt, 2010)

3 HISTORICAL DEVELOPMENT OF MV-PILE TYPE ANCHORS AND THEIR TESTING IN ROTTERDAM

The larger retained height of the quay walls resulted in development of heavier anchors with ultimate bearing capacities increasing from typically 2000 kN in the seventies to the current (estimated) 16000 kN per anchor. From the eighties the maximum test load on MV piles increased from 4000 kN to the current 12000 kN (Fig. 2). The maximum test load is currently limited to 12000 kN due to the axial capacity of the in this application popular HE-600B profiles.

These very high (tension) bearing capacities can be delivered by steel beams installed at 45° and up to 60 m long. The piles are driven with grout injection. The grout is injected at the pile tip through steel buckets welded to the outside of the flanges of the H-beam (Fig. 3).

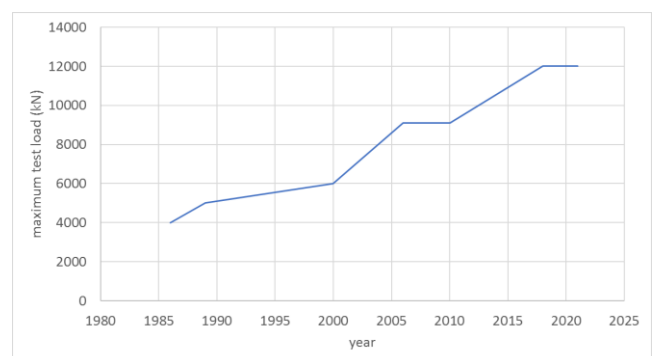


Fig. 2: Test loads on MV piles in Rotterdam through time

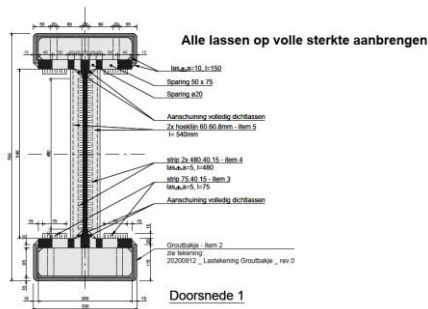


Fig. 3: Cross section of MV pile with grout injection

Load tests were used to empirically determine the relation between CPT cone resistance and ultimate bearing capacity.

Electrical strain gauges were initially used to assess the distribution of axial load along the pile (Fig. 4) as a result of pile-soil friction. The possibilities of those assessments were limited, because of the vulnerability of the strain gauges (particularly the communication cables). In practice, between 25% and 50% of the sensors were damaged after pile installation. The best results were obtained when the strain gauges and the cables were installed in the grout tubes right after the pile driving ended. The internal diameter of the grout tubes posed a practical limit to the number of sensors to about 4 observation levels.

With the limited information available, the engineers of Rotterdam Public Works were still able to come forward with a practical design code. The proposed design method defines 1.4% of the cone resistance as the local peak friction, applied to the shortest outer circumference of the beam, including the grout injection buckets. The design local friction should not exceed 250 kPa. This is equivalent to limiting the cone resistance to 18 MPa. This limit had been introduced because the local soil conditions from the test site did on average not exceed those cone resistance values.

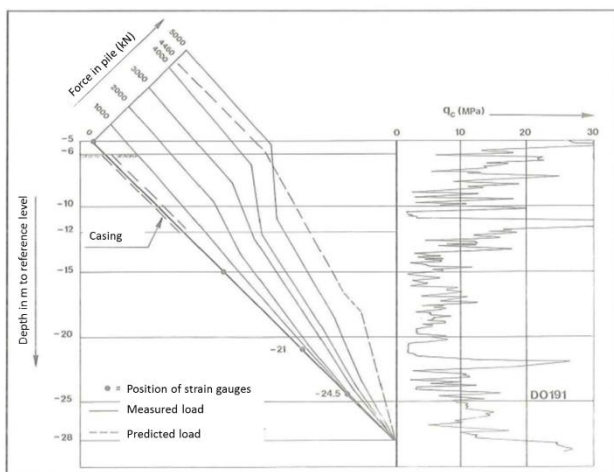


Fig. 4: Axial force determination using electrical strain gauges (Brassinga 1987)

4 PILE INSTRUMENTATION

With the development of Brillouin Optical Time Domain Reflectometry sensor techniques, the opportunities to measure the axial strain in the H-beam increased. In 2006, for the first time the continuous strain profile along an MV pile was measured during test loading up to 9,100 kN using a single optical fibre installed in the grouting tube after pile installation (Fig. 5).

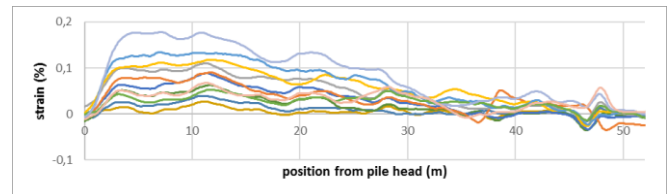


Fig. 5: Axial strain measurement with BOTDR in 2006

Measurement time was around 30 minutes for a profile with a spatial resolution of 1 m and a strain resolution of 50 microstrain. The load tests had an approval test status. It was not intended to load the piles up to geotechnical failure, as can be clearly seen by the very low strains below 35 m from the pile head.

In 2018, at the site in the Mississippihaven port basin (site 1), 6 MV piles were tested to geotechnical failure. These piles were instrumented with fibre optic cables and interrogated with the Omnisense Dual in BOTDA (Brillouin Optical Time Domain Analyses) mode, leading to interrogation times of around 1 minute per sensor, a strain resolution of around 5 microstrain with a spatial resolution of 0,25 m (Fig. 6).

Since the sensor cables were configured in a loop (running from the pile head to the pile tip and back again to the pile head), the spatial resolution was improved by roughly a factor 2 (physical oversampling).

In Fig. 7, the strain starts at the pile head on the left, running down to the pile tip at 150 m sensor position and running up to pile head level again at the right of the graph.

Each strain profile represents a load step during the test.

Around each test pile a casing (steel tube) was installed from surface level (position 110 m) to sensor position 143 m (and from 157 m to 189 m) after H-Pile installation. The purpose of the casing was to detach the upper soil layers from the MV pile. As a result, a larger effective load will act on the deep sand layers where the quay wall will mobilize bearing capacity after dredging the harbour basin.

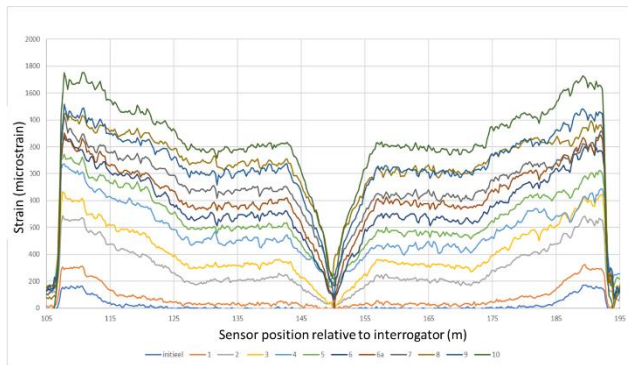


Fig. 6: Axial strain measurement with BOTDA in 2018

While the fibres in 2018 were attached to the H600B beam with epoxy, in 2021 a successful switch to UV-curing cyanoacrylate glue was introduced, reducing curing time from hours to seconds, using a strong UV lamp. Performance-wise the cyanoacrylate glue achieved a similar high-quality bond as compared to the epoxy. In both cases, the glued fibre was mechanically protected by welded-on steel profiles covering the fibre and the glue. The current best practice is:

- removing surface roughness with a grinder;
- put the fibres in the required position;
- apply the glue;
- cure the glue with a UV lamp;
- weld the protective steel profiles (welds not closer than 3 cm to the fibres).

Keep in mind that due to the huge accelerations during pile driving (up to 300 g), everything with mass (inertia) will come off if not properly attached.

Use at least 2 meters sensor cable overlength on both ends of the sensor cable, to allow for splicing in the field. Pre-installed pig-tail cables with connectors are often damaged during pile driving. Expect that roughly half of the connectors will need replacement. Use an easy to clean simple connector type without tiny mechanical parts that will have problems with sand and dust. Accept that dust will be there and that you will have to (thoroughly) clean all connectors before attaching to the interrogator. In the field the SC-APC connectors have performed well.

For axial load in the beam, the fibres must be attached in the centre line of the beam. The flanges can be instrumented additionally if there is an interest in the bending behaviour of the beam. For best performance of the sensors it is highly recommended to do the instrumentation in a clean, constant temperature environment (preferably not in the open air of a building site, although this has been done successfully on site 1). It is important to record the initial strain profile and at the same time the temperature along the structural element that is instrumented. For example, if you want to record the internal stresses in the element due to pile driving, initial strain and temperature correction will be required in most cases.

For axial load in the beam, the fibres must be attached in the centre line of the beam. The flanges can be instrumented additionally if there is an interest in the bending behaviour of the beam. For best performance of the sensors it is highly recommended to do the instrumentation in a clean, constant temperature environment (preferably not in the open air of a building site, although this has been done successfully on site 1). It is important to record the initial strain profile and at the same time the temperature along the structural element that is instrumented. For example, if you want to record the internal stresses in the element due to pile driving, initial strain and temperature correction will be required in most cases.

5 TEST SETUP

The test used a frame to redirect the reaction force into adjacent piles of the same type, skipping 1 pile in the row. On top of the beams, in total 4 hydraulic jacks with load-cells are installed (see Fig. 8). The test pile is extended above the reaction beams. The crossbeam above the reaction beams is pushed away from the reaction beams using the hydraulic jacks.

On 4 positions around the test pile, displacements are measured relative to a reference frame (aluminium truss, which is monitored during the test with a theodolite).



Fig. 7: Reaction frame, test pile in the centre, left reaction pile not visible, right reaction pile on the right in the picture.

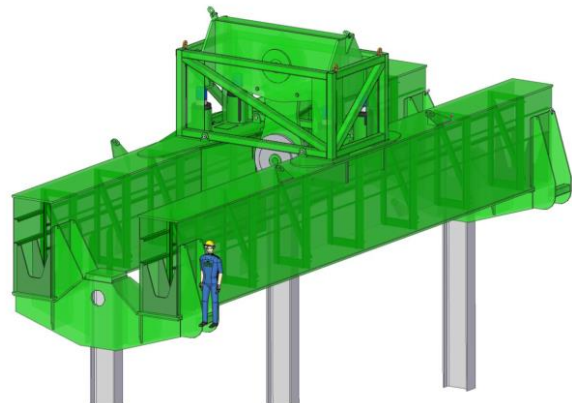


Fig. 8: Scale indication of the test frame

6 TEST RESULTS

The typical output of a load test is the load-displacement curve. It is good practice to show the displacement in the actual direction (so upward for a tension load test and downward for a compression load test).

As a typical example, the test results from site 2 (SIF/OTR quay wall extension Maasvlakte Rotterdam) obtained at June 5th 2021 will be shown in Fig. 9. During the load step at 11459 kN, the amount of creep increased, shown by the 10 mm pile head displacement from 80 mm to 90 mm. After releasing the load to the initial value of 900 kN and reloading again, the pile showed post-peak behaviour with a decreasing capacity with increasing displacement. Post-peak bearing capacity was for this pile 93% of the peak value.

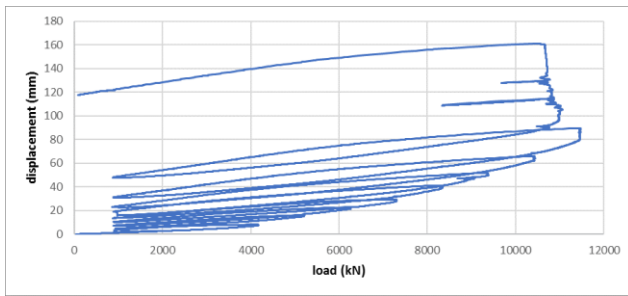


Fig. 9: Load-displacement curve for test pile MV1, tested on the 5th of June 2021.

During the load tests the creep ratio k was used as an indicator of progress towards failure.

Creep ratio k is defined as:

$$k = \frac{\delta_1 - \delta_2}{\log(t_1) - \log(t_2)}$$

In which:

δ_1 is the pile head displacement in mm at t_1 (in minutes from start load step)

δ_2 is the pile head displacement in mm at t_2 (in minutes from start load step, in which t_1 is later in time than t_2)

The resulting k is in mm. Analysing many load tests has shown that up to a creep ratio k of less than 1 mm, geotechnical failure is unlikely to occur. With a k of approximately 2 mm, geotechnical failure is about to occur. Between $k = 1$ mm and $k = 2$ mm, decreasing the load step size is recommended to be able to determine the actual point of geotechnical failure more accurately. In this case, a reduced loadstep size was not implemented because of the decreasing k towards the end of the load step.

The k is best observed over the last half of the load step. For a load step of 1 hour, calculate the k using $t_1 = 60$ minutes and t_2 is 30 minutes with the corresponding displacements. During the load step k may be regularly checked to keep track of creep behaviour (see Table 1). Stabilising creep will show a decreasing k further along the load step. Progressive failure will show itself in an increasing k value. When a decreasing k is observed, prolonging the load step makes sense.

Table 1: Development of creep ratio k per load step

Load step	Load (kN)	Creep ratio 'k' (mm)	Observation interval
[#]	[kN]	[]	[min]
1	2083	0.1 / 0.07	5-15 / 15-30
2	4167	0.8 / 0.63	5-15 / 15-30
3	5209	0.84 / 0.46	5-15 / 15-30
4	6250	0.61 / 0.43	5-15 / 15-30
5	7292	0.85 / 0.33	5-15 / 15-30
6	8333	1.35 / 0.84	5-15 / 15-30
7	9372	0.42 / 1.13 / 0.9	5-15 / 15-30 / 30-60
8	10417	1.84 / 1.89 / 1.45	5-15 / 15-30 / 30-60
9	11459	5.83 / 4.09 / 3.19	5-15 / 15-30 / 30-60
10	10420	53.39 / 15.45 / 40.18 / 85.36	5-15 / 15-30 / 15-45 / 30-60

7 ANALYSES

The primary interpretation uses the strain profile recorded at the end of the last stable load step or the load step at which progressive failure was starting to take place. In the above example, the 11459 kN load step was used, because, even though showing very high values for k , the decreasing trend of k led to the assumption that geotechnical failure was very near but the real failure point was out of reach due to limitations of the axial capacity of the steel cross section.

The recorded strain profile (Fig. 10) shows a high strain peak at sensor position 146 m. This is due to the return loop at the pile tip that consists of a different optical fibre with a different Brillouin scatter frequency. The casing around the pile from sensor position 113 to 139 and 153 to 180 has not succeeded in detaching the pile from the soil friction as intended. Presumably sand and grout inside the casing formed a coupling interface between the casing and the pile. As a result, the observed strain in the pile itself is lower than above and below the casing because the steel cross section of the casing is cooperating with the cross section of the pile, thus lowering the measured strain in the pile. For the interpretation of the bearing capacity we will only use the section between sensor position 139 m and 153 m (the part of the pile below the casing).

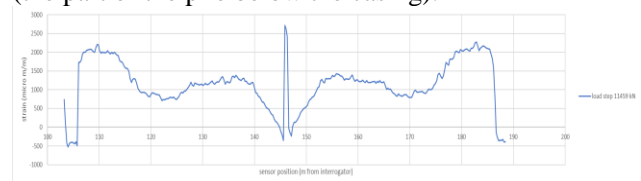


Fig. 10: Raw strain profile recorded at 11459 kN (with BOTDA technology in 2021)

Removing the peak caused by the return loop, averaging both (running down and up) parts of the fibre and adjusting the absolute strain values such that a zero reading is obtained outside the pile (sensor positions 104-106 m and 187-189 m in Fig. 10) and multiplying by the axial stiffness of the pile, we construct Fig. 11 from the data presented in Fig. 10.

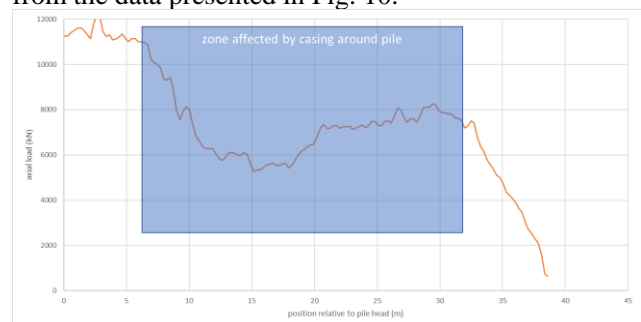


Fig. 11: Axial load profile, derived from strain profile

For further interpretation only the part further than 32 m from the pile head will be used.

This part is shown in Fig. 12, corrected for depth to reference level (using pile-head level and pile

inclination). The average qc (cone resistance) is 47 MPa.

The original design code (orange line in Fig. 12) would clearly lead to an underestimation of the bearing capacity due to the limiting value of local friction of 250 kPa. A 1.2% qc estimation without limiting value (grey line in Fig. 12)(Westerbeke 2021) would in this case have led to an overestimation.

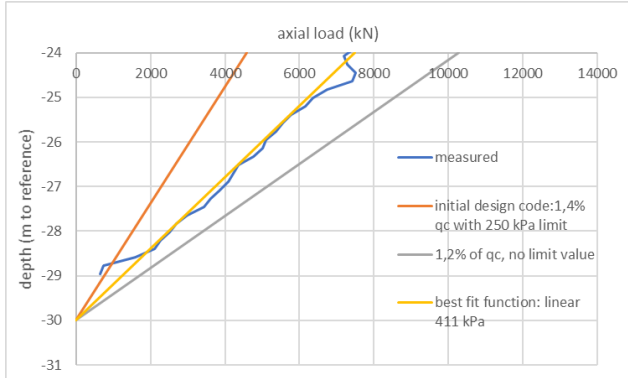


Fig. 12: Measured and modelled axial loads below the casing

The change in axial load along the pile can be directly addressed to local friction which leads to the results shown in Fig. 13. The measured values (blue dashed line in Fig. 13) need filtering to find a trend. In this case a moving average along 3 m pile length was used (red line in Fig. 13). For reference the constant 411 kPa from Fig. 12 has been added, together with 1% of qc.

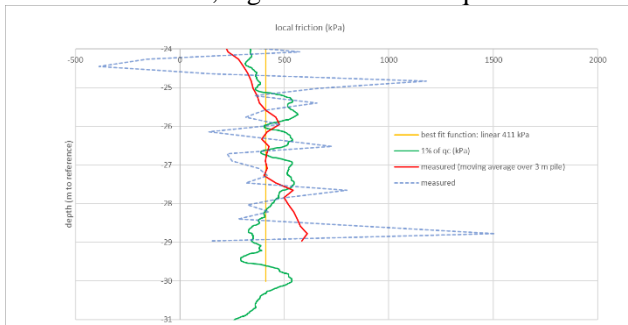


Fig. 13: Local friction derived from strain measurements, combined with 1% qc

As shown in Fig. 13, the strain profile derived local friction does not show a convincing correlation with cone resistance, though around 1% of the cone resistance does not look too bad. The lower than average friction in the upper region and the higher than average friction in the lower part might be the result of the not simultaneous mobilisation of the friction. At failure, the lowest part of the pile may have a higher local friction because the upper part might already be experiencing post-peak softening.

Similar results can be obtained if the local friction is plotted instead of 1% qc, as shown in Fig. 14.

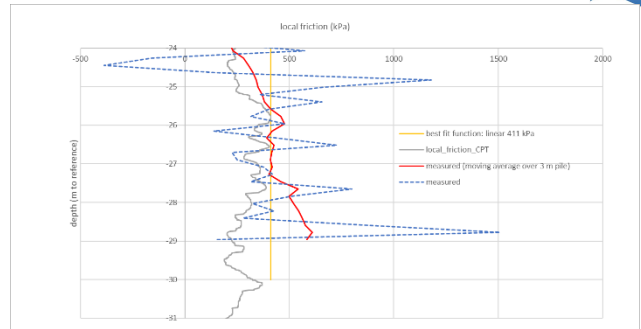


Fig. 14: Local friction derived from strain measurements, combined with CPT determined local friction

If the test results, simplified to average peak friction (in kPa), are plotted against average qc for the two sites with in total 7 tests to geotechnical failure, we find a poor correlation ($R^2 = 0,438$) between cone resistance and peak friction with the expressed linear function (blue dashed line) in Fig. 15.

The previously mentioned 1% qc function (see Fig. 13) also runs decently through the data points (green dashed line Fig. 15), thus avoiding bearing capacity at zero qc.

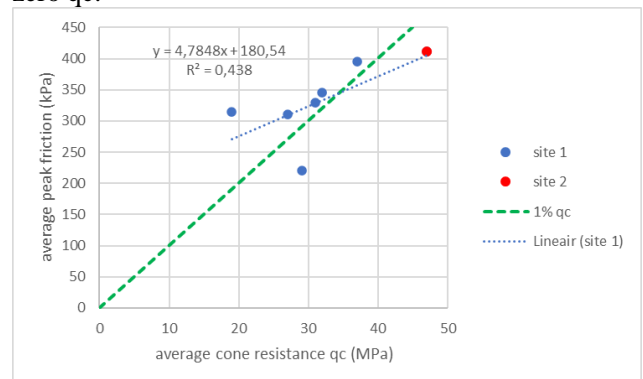


Fig. 15: Average peak friction (kPa) versus average cone resistance qc (MPa)

No reliable test data is available for low qc values, since these MV piles generally mobilise their bearing capacity in a dense sand layer. It seems, however, plausible that in a sand layer, even at very low qc values, the peak friction might not be zero. Due to the pile driving energy, densification of the sand around the pile will occur. The cone penetration tests from the design phase will show the qc before pile installation. Low relative density sand layers will benefit more from this densification effect than (very) dense soil layers. Extremely dense sands might even lose some density (and as a result bearing capacity) due to the piling vibrations. Possibly, the truth is somewhere between the dashed blue and green lines of Fig. 15. Or more likely, the relation between qc and peak friction is a non-linear curve.

For future tests, it is recommended to also include testing the bearing capacity in the lower qc range to verify the above hypothesis. In addition to that, dividing the length of the pile in multiple parts, will lead to more

data points for the graph in Fig. 15 and might give better understanding of the relation between q_c and friction.

Based on these tests, 1% of the q_c seems a proper predictor for peak local friction.

The test results have shown that some averaging of the strain and cone resistance should be applied to filter the otherwise too large variations. In this case averaging the strain over 3 m pile rendered the best compromise.

Another option worth investigating, is the correlation with the measured local friction in the CPT. Although the local friction measurement is often considered less reliable compared to the cone resistance, the friction sleeve will directly deliver the local friction in kPa. The influence of grouting the pile and the dynamic aspects of pile driving will influence the peak friction along the pile, but might be corrected in a factor.

On test site 2, a factor of 1.4 between measured CPT local friction and load test peak friction was found. Where $\text{pile_friction} = 1.4 * \text{CPT_friction}$. This idea needs further study and, in case of positive outcome, would imply more accurate friction measurements in CPT testing, for example through more regularly replacing or calibrating the friction sleeve.

In the previous section, the maximum local friction along the pile was addressed. How this friction is mobilised as a function of local displacement has also been analysed using the strain data. By coupling the measured pile-head displacements and the sum of all measured strains along the pile, the physical position of each section of 0,25 m of the pile is known during the test. For each load step, per pile section, the friction and displacement were derived, resulting in mobilisation curves (Westerbeke 2021).

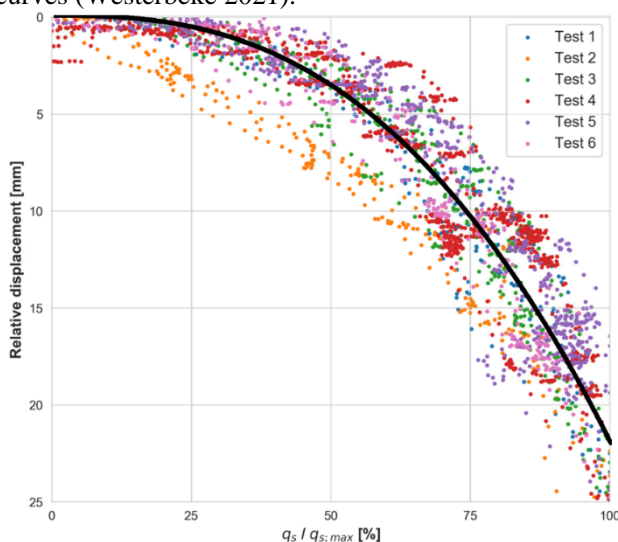


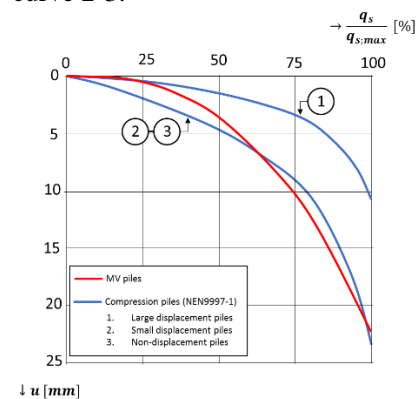
Fig. 16: Mobilisation curve derived from 6 load tests on site 1

The mobilisation curve in Fig. 16 can be modelled using: $y = 22 * x^{2.6}$.

Compared to the mobilisation curves for shaft friction proposed in the Dutch national design code

NEN9997-1, the load-test-derived curve of Fig. 16 does coincide generally with curve 2-3 (see Fig. 17). Up to 30% of the peak friction, the test derived mobilisation curve exhibits the same stiffness behaviour as curve 1. Between 30% and 60% mobilisation of the peak friction, the stiffness behaviour softens to more or less the same as curve 2-3 from the design code.

If a user-defined mobilisation curve can be used in a (finite element) simulation model, the red curve of Fig. 17 is recommended. If only the predefined curves of the Dutch code can be chosen, the best option seems to use curve 2-3.



↓ u [mm]

Fig. 17: Test derived mobilisation curve versus design code NEN9997-1

8 CONCLUSIONS AND RECOMMENDATIONS

Strain measurements using BOTDR or BOTDA interrogation of optical fibres offers a detailed and effective method to determine the axial load in piles during a static load test.

The development of the logarithmic creep factor 'k' through the load steps and in time during a load step, has proven to be very effective in assessing the approach of the limit state of geotechnical failure. As a rule of thumb; $k < 1$ mm: no failure imminent, $1 \text{ mm} < k < 2$ mm: geotechnical failure is near, $k > 2$ mm: the pile is failing (or very close to geotechnical failure).

The tested piles have performed better than expected based on the basis of the Dutch design code. The design code prescribes a linear correlation between cone resistance and peak shear strength with a limit for peak shear friction at 250 kPa.

The test results show that this limit value probably is too conservative. For a proper determination of the function describing the relation between cone resistance and peak shear strength, tests including sand layers with low cone resistance should be executed.

From the test results it is expected that the peak shear strength can be estimated from cone resistance:

$$\text{Peak_shear_strength} = 0,01 * q_c$$

Because the only test currently available for sands



with an average q_c of 47 MPa showed an average peak friction of 411 kPa, a limit value for average peak shear strength in that order of magnitude is recommended.

The glass fibre measured strains also offer the option to determine the peak shear strength over parts of the pile, with lengths of only a few meters. This enables to analyse the test results more in detail and increase the understanding of the relationship between peak shear strength and q_c . It is recommended to do this in cases where also bearing capacity is derived from sand layers with lower q_c values.

A correlation between peak shear strength and CPT derived local friction (measured with the friction sleeve above the cone) was observed at test site 2, showing on average:

$$\text{Peak_shear_strength} = 1,4 * \text{CPT_local_friction}$$

It is worth investigating if this is also encountered in other test sites.

For modelling the mobilisation of the shear resistance along the pile, the mobilisation curve as described in this paper can be used. If simulation according to the predefined curves of the Dutch design code is required, curve 2-3 for small- or non-displacement piles is recommended.

REFERENCES

- 1) Brassinga, H.E. (1987), Proefbelasting van twee m.v.-palen aan de britanniëhaven te rotterdam. Technical report, Gemeentewerken Rotterdam.
- 2) De Gijt, J.G. (2010), A History of Quay Walls: Techniques, types, costs and future.
- 3) Nederlands Normalisatie-instituut (2017), Geotechnisch ontwerp van constructies - Deel 1: Algemene regels/Geotechnical design of structures - Part 1: General rules.
- 4) Nederlands Normalisatie-instituut (2017), Nederlandse praktijkrichtlijn. NPR 7201 - Determination of the axial bearing capacity of foundation piles by pile load testing.
- 5) Putteman, J., Broos, E.J., Brassinga, H.E., Spruit, R., De Vos, M., and Timmermans, A.L.J. (2019), MV tension pile load tests in the port of rotterdam: practical aspects and geotechnical behaviour. Proceeding of the European Conference on Soil Mechanics and Geotechnical Engineering, Reykjavik.
- 6) Westerbeke, F.Y.H. (2021), Geotechnical bearing capacity of MV piles, Improving the design based on full scale load tests in the port of Rotterdam.